

# Thermal Resistance Analysis of Flexible Composites Based on $\text{Al}_2\text{O}_3$ Aerogels

Jianzheng Wei, Duo Zhen, Zhihan Yang, Huifeng Tan

**Abstract**—The deployable descent technology is a lightweight entry method using an inflatable heat shield. The heatshield consists of a pressurized core which is covered by different layers of thermal insulation and flexible ablative materials in order to protect against the thermal loads. In this paper, both aluminum and silicon-aluminum aerogels were prepared by freeze-drying method. The latter material has bigger specific surface area and nano-scale pores. Mullite fibers are used as the reinforcing fibers to prepare the aerogel matrix to improve composite flexibility. The flexible composite materials were performed as an insulation layer to an underlying aramid fabric by a thermal shock test at a heat flux density of  $120 \text{ kW/m}^2$  and uniaxial tensile test. These results show that the aramid fabric with untreated mullite fibers as the thermal protective layer is completely carbonized at the heat of about 60 s. The aramid fabric as a thermal resistance layer of the composite material still has good mechanical properties at the same heat condition.

**Keywords**—Aerogel, aramid fabric, flexibility, thermal resistance.

## I. INTRODUCTION

INFLATABLE decelerator is known as inflatable heatshield, of which a durable high temperature capable outer layer required to protect the underlying layers [1], a resistance layer required to mitigate the high temperature of the outer surface to a temperature that the heatshield can tolerate. The decelerate technology is attractive for a variety of entry mission such as planetary mission [2]. Therefore, it is necessary to study the flexibility and thermal resistance of the thermal insulation layer on the windward side. Most of the pressurized materials performed aero-braking at subsonic speed are flexible, high-strength Kevlar<sup>®</sup> fabrics which exhibit low temperature resistance and carbonize at about  $400^\circ\text{C}$ , resulting in loss of mechanical properties. Therefore, a lightweight, foldable, high temperature insulation is required to protect it. Many efforts have been proposed on the insulation for flexible materials.

A relatively perfect thermal protection system has been performed in 2000, and this thermal insulation named MLI had undergone thermal vacuum test and simulated thermal load test, the experimental results showed that MLI was found to be a very effective heat-resistant material [3]. NASA used Nextel/Pyrogel/Kapton<sup>®</sup> ply for thermal protection of

inflatable decelerator [4], the thermal insulation layer Pyrogel 3350 is a thermal insulation blanket which is effectively combined by hydroxyl and micro-glass fiber; and the Nomex weave fibers coated with Viton<sup>®</sup> were also adopted to verify the scheme by an experiment [5]. Foelsche et al. [6] studied the heat resistance of flexible fabrics at speeds less than 4 Mach. In view of the strength and tightness testing of flexible fabrics, Hutchings et al. [7] proposed a method for tensile/torsion testing of fabric composites based on Turner's theory [8], and carried out the performance testing of four kinds of textile materials, including two silicone coated para-aramid synthetic layups, an aromatic polyester, and a proprietary material. Boulware et al. [9] designed a multilayered material with high thermal emittance, which is composed of a fabric containing a preimpregnated ceramic polymer as well as a living filler, this material can evaporate and cool the high temperature material.

Nano-porous aerogels have become the most promising thermal insulation materials and attracted extensive attentions for their extremely low thermal conductivity and low density. Schüßler et al. [10] conducted the heat flux of  $\text{Al}_2\text{O}_3$  and high temperature creep experiments of alumina aerogel. Thermogravimetric analysis illustrated that depositing the  $\text{Al}_2\text{O}_3$  nanolayer on the surface of the fibers had the effect of resisting high-intensity UV-induced mechanical strength damage [11]. In order to improve the abrasion resistance of textiles, nano-coatings can be deposited on the surface of textiles using  $\text{Al}_2\text{O}_3$  sol-gel method [12], [13]. In addition, Aboshio et al. [14] conducted tensile strength tests and expansion test of neoprene-coated nylon fabric composites at different temperatures. Studies on thermal protection ablation materials found that alumina and aluminosilicate aerogels have great application value at temperatures above  $700^\circ\text{C}$ . Hurwitz et al. [15] studied a structure of alumina and aluminosilicate aerogels, achieving better high temperature performance. Moreover, researches on the additional effects of different nanoparticle resins on the mechanical properties of coated fabrics have made some progress [10].

In this paper, firstly, a bulk silicon-aluminum composite aerogel was prepared with nano-scale pores by freeze-drying method. Then, mullite fibers were used as the reinforcing fibers to prepare this aerogel matrix. Finally, thermal resistances of the flexible silicon-aluminum aerogel composites were tested, in order to assess the thermal shock performance as an insulation layer added to the aramid fabric.

## II. PREPARATION OF AEROGEL MATERIALS

This paper adopts alumina aerogel with great heat resistance

Jianzheng Wei is with the Center for Composite Materials and Structures, Harbin Institute of Technology, Harbin, 150080 China (corresponding author, phone: +86-451-86403612; fax: +86-451-86403612; e-mail: weijz@hit.edu.cn).

Huifeng Tan is with the Center for Composite Materials and Structures, Harbin Institute of Technology, Harbin, 150080 China (e-mail: tanhf@hit.edu.cn).

and thermal insulation performance as a thermal insulation material. Taking into account the poor flexibility of aerogel materials, so using the mullite fibers with good heat resistance as a reinforcement phase, and the thermal resistance layers of alumina aerogel composites and aluminum-silicon aerogel composites were prepared respectively. The preparation process mainly includes sol-gel preparation, aging and drying. In this paper, aerogels are prepared by sol-gel methods, which are divided into the particle method and the polymerization method. During the experiment, it was found that the strength of the alumina aerogel prepared by the polymerization method is too low to combine well with the mullite fibers. However, the alumina aerogel prepared by the particle method can combine nicely. Therefore, in this paper, the particle method was used to prepare the alumina aerogel, and the polymerization method was used to prepare the aluminum-silicon aerogel.

#### A. Preparation of Alumina Aerogel

In the process of preparing alumina sol by particle method, ASB (Aluminum sec-butoxide) was used as precursor, deionized water as solvent and nitric acid as catalyst. During the hydrolysis of the particle method, ASB is more sensitive to pH of the solution. Meanwhile, the concentration of ASB has a greater impact on the stability of the hydrolysis. In the particle method, this paper chooses ASB:H<sub>2</sub>O as 1:28, uses nitric acid with pH 0.2 to adjust the PH of solution to 5, heats in the water bath of 90 °C, and hydrolysis for 7 hours with 400 r/min stirring speed, then the stable alumina gel can be obtained after standing for a period of time, as shown in Fig. 1 (a); standing it for 24 hours for aging to enhance the strength of the gel skeleton; then the gel was placed in an environment at -25 °C for freezing, finally freeze-dried in a freeze dryer to obtain an alumina aerogel, as shown in Fig. 1 (b).



Fig. 1 Samples of (a) alumina gel (b) alumina aerogel

The four main peaks in the XRD image shown in Fig. 2 are all Boehmite ( $\gamma$ -AlOOH) diffraction peaks, indicating that the alumina aerogel structure obtained by the particle method is a polycrystalline Boehmite structure; as can be seen from the adsorption-desorption curve in Fig. 3, the isotherm is type IV, indicating that the pore size in the structure is mainly mesoporous, and the hysteresis loop is type H3, illustrating that the structure is mainly sheet particles. The measured specific surface area of the sample is 330.5 m<sup>2</sup>/g representing a larger a larger specific surface area, indicating that the

material contains many internal pores as a porous material. Its average pore size is 5.146 nm, the pore is mesoporous (2~50 nm), the pore size is far less than the free path (69 nm) of air molecules, so the material has good thermal insulation properties.

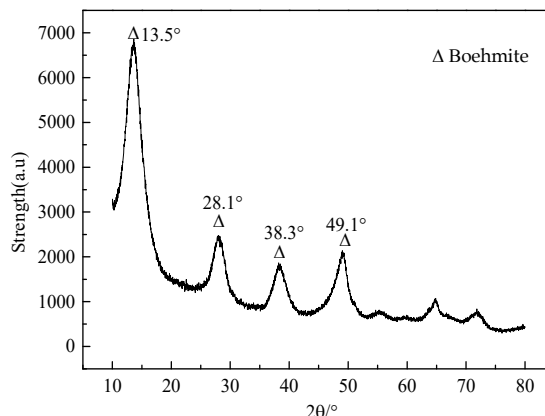


Fig. 2 XRD image of alumina aerogel

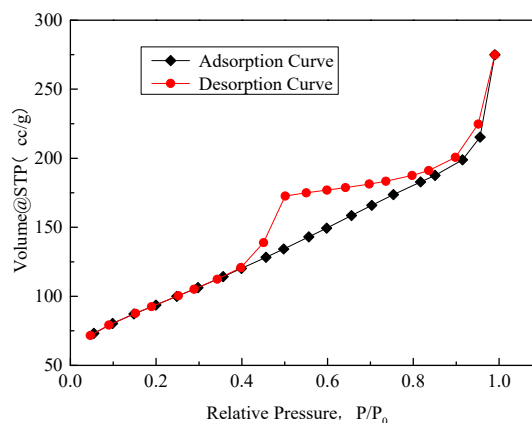


Fig. 3 Adsorption-desorption curve of alumina aerogel

#### B. Preparation of Aluminum-Silicon Aerogel

Similar to the preparation of Al<sub>2</sub>O<sub>3</sub> aerogel, a silicon-aluminum aerogel was prepared by freeze-drying using polymerization method. Here, the molar ratio of ASB, ethanol and deionized water was chosen as 1: 12: 1.2. In order to prepare the Al<sub>2</sub>O<sub>3</sub> solvent, the water bath heating was at 60 °C with stirring rate at 400 r/min. The molar ratio of TEOS, ethanol and deionized water was set as 1:4:1. The clarified and stable SiO<sub>2</sub> solvent was obtained after magnetic stirring for two hours at room temperature. The two sols evenly were stirred to get a stable mixed sol liquid. A small amount of aqueous ammonia is added dropwise to the solution to promote gelation, where the ratio of Al to NH<sub>3</sub> is 1: 0.003. Using the deionized water and tert-butanol mixture to replace the solvent, where the mass ratio of them is 4: 1, after 48 hours of freeze-dried, and the aluminum-silicon aerogel can be obtained. Al and Si sols with different molar ratios were mixed respectively. After the sol-gel with the molar ratio

between 2: 1 and 3: 1 was dried, the aluminum-silicon aerogel, as shown in Fig. 4, can be obtained with better lumpiness and higher strength.



Fig. 4 The sample of aluminum-silicon aerogel

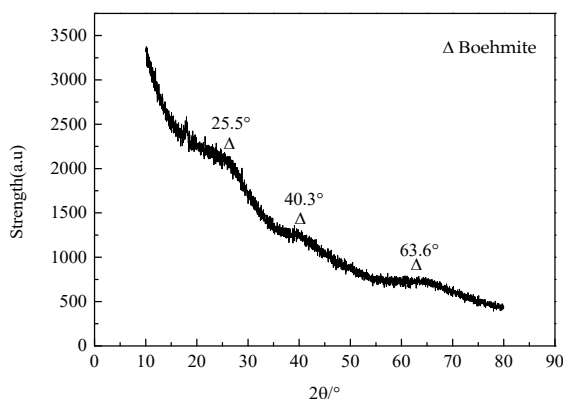


Fig. 5 XRD image of aluminum-silicon aerogel

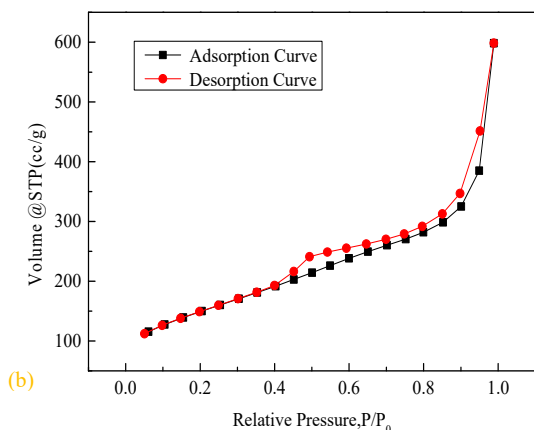


Fig. 6 Adsorption-desorption curve of aluminum-silicon aerogel

As shown in Fig. 5, there is no obvious diffraction peak in the XRD image, indicating that there is no larger crystal in the aerogel structure because of the large amount of silicon in the alumina aerogel and the partially incompletely hydrolyzed Butyl and Ethyl, these components hinder the formation of alumina crystals. From the adsorption-desorption curve in Fig. 6, the type of isotherm is IV, indicating that the pore size in the structure is mainly mesoporous (2 to 50 nm). The hysteresis loop is H3 type, illustrating that there was a lamellar

granular structure within the material. The measured specific surface area of the sample is 529 m<sup>2</sup>/g. The average pore size is 7.00 nm, which is much smaller than the free path of air molecules. Therefore, the material has good thermal insulation properties.

#### C. Preparation of Flexible Thermal Layer

Nanoporous Al<sub>2</sub>O<sub>3</sub> aerogels have lower density and higher porosity. Therefore, nanoporous Al<sub>2</sub>O<sub>3</sub> aerogels theoretically have lower thermal conductivity and higher heat resistance; hence, it is an ideal thermal insulation material. However, at the same time, the low density and high porosity of Al<sub>2</sub>O<sub>3</sub> aerogels lead to its low strength, high brittleness and poor lumpiness, which cannot meet the requirements of the flexible insulation layer of inflatable decelerator. Therefore, this paper adopted the high temperature mullite fibers insulation mat (80% Al<sub>2</sub>O<sub>3</sub>, 20% SiO<sub>2</sub>) as the reinforcement phase to prepare the nanoporous Al<sub>2</sub>O<sub>3</sub> aerogel composite insulation layer. The free path of air molecules is about 69 nm, and the spacing of fibers inside mullite fibers insulation mats is 30~100 μm. Therefore, the sol-impregnation method is used in this paper to allow the sol to fill the interior of mullite fibers with good flowability, and then make it gel, after drying. We can get nanoporous Al<sub>2</sub>O<sub>3</sub> aerogel composite material. In the impregnation process, if the sol is injected too much, there will be a large number of powdery materials that easily fall off on the surface of the sample after drying, which is not conducive to the follow-up observation and thermal shock resistance experiment; if the sol is injected insufficiently, during gelation and aging, the gel would crack due to the evaporation of the solvent. Therefore, during the impregnation process, the sol liquid surface should just pass over the upper surface of the fiber, which can prevent excessive powdery material on the surface of the sample after drying and can also effectively prevent gel cracking in the sample. The obtained alumina aerogel composites all have good flexibility and certain elasticity, as shown in Fig. 7.



Fig. 7 (a) Nanoporous Al<sub>2</sub>O<sub>3</sub> aerogel composites prepared by particle method (left: original sample; middle: compressed sample; right: recovery sample), (b) Aluminum-silicon aerogel composites with reinforcement phase of mullite fibers (left: original sample; middle: compressed sample; right: recovery sample)

In the alumina aerogel composites obtained after drying, the mass of the composites is 1.5 times the mass of the mullite

fibers. As can be seen from Fig. 8 (a), the alumina aerogel combines well with the mullite fibers but fails to completely fill the pores of the mullite fibers; in contrast, aluminum-

silicon aerogel composites bond well with mullite fibers and almost fill the pores of the mullite fibers completely in Fig. 8 (b).

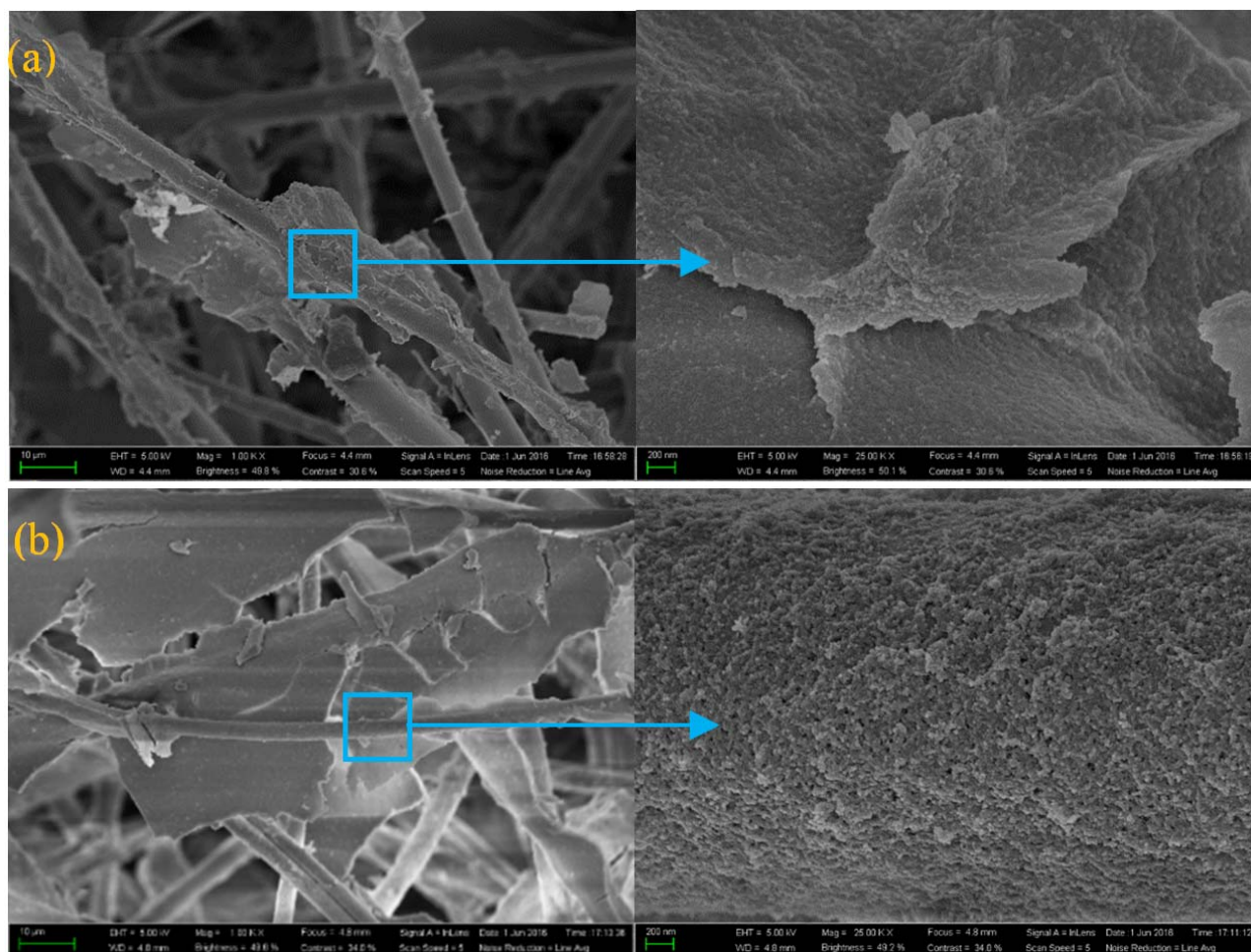


Fig. 8 Microstructure of (a) nanoporous  $\text{Al}_2\text{O}_3$  aerogel composites (b) aluminum- silicon aerogel composites

### III. TEST OF THERMAL SHOCK RESISTANCE

#### A. $\text{Al}_2\text{O}_3$ Aerogel/fabric Flexible Materials

Kevlar® textile is made of aramid fabric material. The fabric weaving structure is different, even if the fiber yarn is the same; the mechanical properties of the textiles are also different. Aramid textiles are usually anisotropic, at least to study the performance of the warp and weft directions and even the thickness direction. Due to the flexibility of the yarn itself and the lack of strong connection between the yarns, displacement of the fibers and yarns occurs as the fabric deforms. Therefore, different test methods will affect the test results of the tensile properties of fabric materials. In this paper, based on the previous studies, the tensile samples are prepared by the Split-Edge method. As shown in

Fig. 9, the width of the cutting sample is 10 mm more than the specified width (40 mm) of the effective sample, and then the yarn is removed from both sides of the sample in the width

direction by Split-Edge method until the width of the sample meets the specified requirements, guaranteeing that there are 38 bundles of fiber, to ensure that during the test the yarn will not emerge from the flash, and clamping along the width direction of the samples.

Due to the textile material of Kevlar® fabric, the clamping of common stretching equipment cannot meet the requirement of textiles, so special treatment of aramid textiles holding end is needed. As shown in Fig. 10, 40 mm  $\times$  50 mm thin aluminum sheets were pasted 40 mm from the front end of the samples by using an adhesive, the remaining 40 mm wide fibers were folded and pasted on the thin aluminum sheet, after the adhesive curing, fold the sample again, and paste another thin aluminum sheet on the back end of the aramid sample. These samples were tested by the uniaxial tensile in order to make the textiles uniformly stretched by this method, which effectively avoid the fibers from slipping and falling off at both ends.



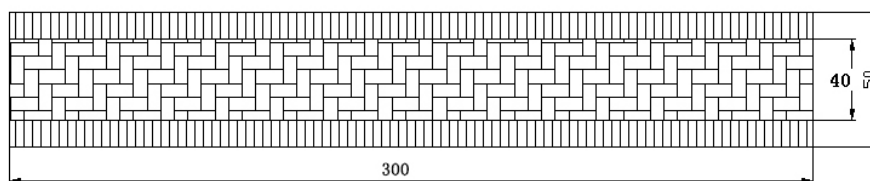


Fig. 9 Aramid textiles samples (Unit: mm)

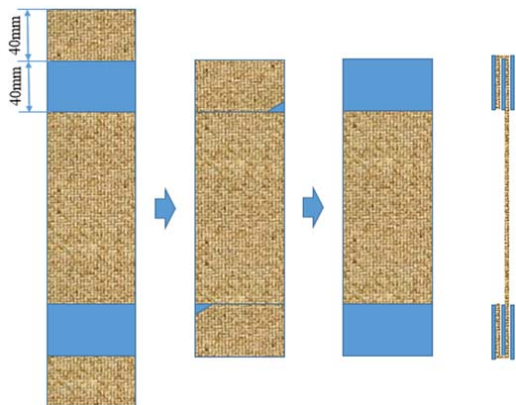
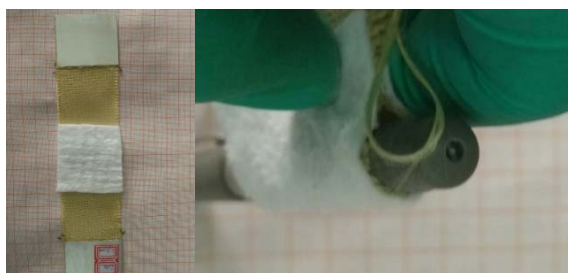


Fig. 10 Schematic of reinforcing the both end of the tensile sample

The insulation layer and the aramid fabric are combined by bonding. The “Iron Anchor” adhesive with strong cohesive force is used for bonding. The mass ratio of the adhesive to the curing agent is 100:24. Because of the weak adhesion ability of  $\text{Al}_2\text{O}_3$  aerogel in the aerogel composite prepared by the polymerization method, the particles are easy to fall off, which is unfavorable to the bonding. Therefore, the aerogel composite material prepared by the particle method and the aluminum-silicon aerogel composites are tested for adhesion. As shown in Fig. 11, the bonded material has good flexibility.

Fig. 11  $\text{Al}_2\text{O}_3$  aerogel/fabric flexible materials

### B. Test of Thermal Resistance

A thermal shock was tested by a butane burner. Testing conditions are following: a butane burner was used to conduct thermal shock test on pure aramid and aramid with thermal insulation layer. Testing conditions are following: the covers with thermal resistance lay are vertically ablated with the flame, controlling the ablation area about 20 mm in diameter, and the flow density on the sample cover remained consistent at  $120 \text{ kW/m}^2$  and the duration is 60 s. The thermal shock condition simulates the heat flow environment during reentry.

In this paper, pure aramid fabric, aramid fabric with 0.40 g Mullite fibers insulation mat as insulation layer, aramid fabric with insulation layer of  $\text{Al}_2\text{O}_3$  aerogel composites prepared by the particle method and Mullite fibers reinforced aluminum-silicon aerogel composites are selected to conduct the thermal shock experiment, respectively. In the experiment, at a heat flux density of  $120 \text{ kW/m}^2$ , the pure fabric started burning at the moment of contact with the heat flow; the samples with 0.40 g pure mullite fibers insulation material as insulation layer started to burn when ablation continued for 39 s. As shown in the first row of Table I, it is a sample of the fabrics with insulation layer of  $\text{Al}_2\text{O}_3$  aerogel composites prepared by the particle method, the mass of the insulation mats before impregnating with sol was 0.23 g, no burning occurred after ablation of 60 s, but a certain amount of smoke appeared. The center of the sample was completely carbonized at the ablation site and the carbonization site lost its toughness. As shown in the second row, the fabric sample with insulation layer of the aerogel composites, the mass of the insulation mats before impregnating with sol was 0.68 g, on which appeared the same phenomenon. Using a new sample of aramid fabric with insulation layer of Mullite fibers reinforced aluminum-silicon aerogel composites for ablation whose insulation mats before impregnating with sol weighed 0.37 g, burning also did not occur after ablating for 60 s, but a certain amount of smoke appeared. The ablation center of the sample also occurred carbonization, but the carbonized area was smaller than the first two groups; part of the fiber became dark yellow, its surface appeared carbonation, but still had some flexibility, as shown in the third row of Table I. Using another fabric sample with insulation layer of mullite fibers reinforced aluminum-silicon aerogel composites for ablating the same time, whose insulation mats before impregnating with sol weighed 0.76 g, almost the same phenomenon happened shown in the fourth row of the Table I, however, at the center of the ablation sample, only the surface of the fiber was carbonized, and some of the fibers turned dark yellow but still had good flexibility. Obviously, the ablation results of the fourth sample were better than the first three samples.

### C. Uniaxial Tensile Test

To test the damage of the aramid textiles, we performed a uniaxial tensile test on the aramid textiles after the thermal shock test. The test results are shown in Table II and Fig. 12. Since the ablation site of the sample is in the center of the sample, destruction always occurred in the center when it is pulled. From the load-displacement curve and the residual strength of the tensile samples, it can be seen that the

nanoporous  $\text{Al}_2\text{O}_3$  aerogel composites prepared by the particle method had a certain degree of insulation, and compared with the sample with untreated insulation mat as its insulation layer (the aramid textiles began to burn after 39s), its insulation performance was greatly improved, but the sample was still seriously damaged, and the intensity was reduced to a lower degree; the thickness of the insulation layer obtained by particle method is increased, and the insulation performance is improved, but the degree of improvement is not large. The reason is that the nanoporous  $\text{Al}_2\text{O}_3$  aerogel prepared by the particle method is easily subjected to heat sintering under the high temperature and the phase change occurs, therefore, insulation performance is reduced, resulting in a small difference in insulation performance of different thicknesses insulation layers. The insulation effect of the sample with the

insulation layer of mullite fibers reinforced aluminum-silicon aerogel composites was significantly better than that of the  $\text{Al}_2\text{O}_3$  aerogel composites prepared by the particle method. The reason is that the lumpiness of the aluminum-silicon aerogel composites is better, and the nanoporous aerogel fills the pores in the mullite fibers, which hinders the air flow inside the structure, so that the thermal conductivity of the structure decreases greatly; the thickness of the insulation layer has a greater influence on the insulation capacity. The reason is that the aluminum-silicon aerogel in the insulation layer is still brittle, and the aerogel material adhering to the surface is easy to fall off, and the proportion of the thicker insulation layer is smaller, so it has a higher insulation capacity, meanwhile, the areal density of that material is  $464 \text{ g/m}^2$ .

TABLE I  
ABLATION RESULTS OF THE SAMPLES


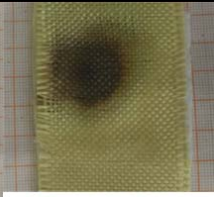


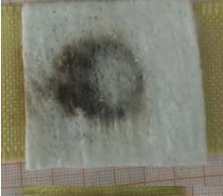
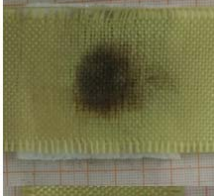

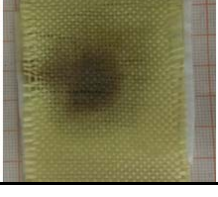
Process parameters	The front of the ablation sample	The back of the ablation sample
$\text{Al}_2\text{O}_3$ aerogel composites prepared by the particle method, Reinforced fibers 0.23 g		
$\text{Al}_2\text{O}_3$ aerogel composites prepared by the particle method, Reinforced fibers 0.68 g		
Aluminum-silicon aerogel composites prepared by the polymerization method, Reinforced fibers 0.37 g		
Aluminum-silicon aerogel composites prepared by the polymerization method, Reinforced fibers 0.76 g		

TABLE II  
RESIDUAL STRENGTH OF TENSILE SAMPLES ABOUT ARAMID TEXTILE

No.	Type of the insulation layers	Fibers mass	Mass of insulation layers	Areal density of insulation layers	Limit load/N	Residual strength rate
1	No treatment without ablating	0 g	0 g	-	2911.98	1
2	Aluminum-silicon aerogel insulation	0.76 g	1.16g	$464 \text{ g/m}^2$	2432.62	0.835
3	Aluminum-silicon aerogel insulation	0.37 g	1.04g	$416 \text{ g/m}^2$	1562.99	0.537
4	$\text{Al}_2\text{O}_3$ aerogel insulation	0.68 g	0.98g	$392 \text{ g/m}^2$	1487.20	0.508
5	$\text{Al}_2\text{O}_3$ aerogel insulation	0.23 g	0.54g	$216 \text{ g/m}^2$	1219.85	0.418

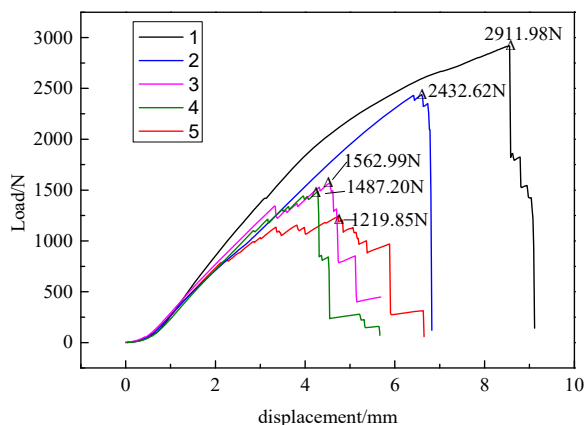


Fig. 12 Load-displacement curve of tensile samples

#### IV. CONCLUSION

In this paper, a lightweight, flexible  $\text{Al}_2\text{O}_3$  aerogel and aluminum-silicon aerogel composite insulation layers were prepared using mullite fibers as reinforcement phase, and the thermal resistances were tested. The findings from the work can be concluded as follows:

- (1) The aluminum-silicon aerogel has better lumpiness and higher strength than the aluminum aerogel, and the former is provided with bigger nanoporous than the latter.
- (2) The  $\text{Al}_2\text{O}_3$  aerogel compounded in mullite fibers can improve the aerogel flexibility after the processes of gelation, aging, drying and folded.
- (3) Mullite fibers composites based on aluminum-silicon aerogel are provided as a flexible insulation layer, which has effective thermal resistance, and mitigates the high temperature as protection for the underlying aramid fabrics.

#### ACKNOWLEDGMENT

This work was supported by the Open Funding of National Key Laboratory of Composite Technologies in Special Environments, China.

#### REFERENCES

- [1] E. H. Richardson, M. M. Munk, B. F. James, "Review of NASA in-space propulsion technology program inflatable decelerator investments," *18th AIAA Aerodynamic Decelerator Systems Technology Conference*, Munich, Germany, May 2005.
- [2] A. M. Korzun, G. F. Dubos, C. k. Iwata, "A concept for the entry, descent and landing of high-mass Payloads at Mars". *Acta Astronautica*, vol.66, pp. 1146-1159, 2010.
- [3] Z. Shen, "Inflatable Re-entry Shield of Payload Recovery Technology," *Spacecraft Recovery & Remote Sensing*, no. 2: pp.1-6, 2001.
- [4] F. Sabri, A. A. Lakis, "Hybrid finite element method applied to supersonic flutter of an empty or partially liquid-filled truncated conical shell," *Journal of Sound and Vibration*, vol.329, no.3, pp. 302-316, 2010.
- [5] G. Xia, W. Cheng, Z. Qin, "Development of Flexible Thermal Protection for System Inflatable Re-entry Vehicles," *Aerospace Materials Technology*, no.6, pp.1-6, 2003.
- [6] R. O. Foelsche, A. A. Betti, R. S. M. Chue, et al. "Supersonic decelerators for freeflight atmospheric flight testing," *17th AIAA International Space Planes and Hypersonic Systems and Technologies Conference*. San Francisco, California, pp. AIAA-2011-2292, 2011.
- [7] A. L. Hutchings, R. D. Braun, K. Masuyama, et al. "Experimental determination of material properties for inflatable aeroshell structures," *20th AIAA Aerodynamic Decelerator Systems Technology Conference and Seminar*. Seattle, Washington, pp. 4-7, 2008.
- [8] A. W. Turner, J. P. Kabche, M. L. Peterson, et al. "Tension/torsion testing of inflatable fabric tubes," *Experimental Techniques*, vol. 32, no.2, pp. 47-52, 2008.
- [9] J. C. Boulware, D. Andrews, B. Bloudek, "Thermally protecting a reentry ballute with transient porosity," *AIAA Space 2007 Conference & Exposition, Long Beach, California*, pp.18-20, September 2007.
- [10] M. Schüßler, M. Auweter-Kurtz, G. Herdrich, et al. "Surface characterization of metallic and ceramic TPS-materials for reusable spacevehicles," *Acta Astronautica*. vol. 65, pp. 676-686, 2009.
- [11] X. Xiao, X. Liu, G. Cao, et al. "Atomic layer deposition  $\text{TiO}_2/\text{Al}_2\text{O}_3$  nanolayer of dyed polyamide/aramid blend fabric for high intensity UV light protection," *Polymer Engineering & Science*. vol. 55, pp. 1296-1302, 2015.
- [12] S. Brzezinski, D. Kowalczyk, B. Borak, "Applying the sol-gel method to the deposition of nanocoats on textiles to improve their abrasion resistance," *J. of Applied Polymer Science*. vol. 125, pp. 3058-3067, 2012.
- [13] J. wei, X. Hou, H. Tan, Y. Liu, "Heat resistance investigation and mechanical properties of fabric coated with  $\text{Al}_2\text{O}_3$  sol-gel," *The Journal of The Textile Institute*, vol.109, no.1, pp.8-16, 2018.
- [14] A. Aboshio, S. Green, J. Ye "Experimental investigation of the mechanical properties of neoprene coated nylon woven reinforced composites," *Composite Structures*. vol. 120, pp. 386-393, 2015.
- [15] F. I. Hurwitz, M. Gallagher, T. C. Olin, M. K. Shave, et al. "Optimization of Alumina and Aluminosilicate Aerogel Structure for High-Temperature Performance," *International J. of Applied Glass Science*. no.5, pp. 276-286, 2014.
- [16] K. Abid, S. Dhouib, F. Sakli, "Addition effect of nanoparticles on the mechanical properties of coated fabric," *The Journal of The Textile Institute*, vol. 101, no.5, pp. 443-451, 2010.

**Jianzheng Wei**, Ph.D in Engineering Mechanics, Harbin Institute of Technology (HIT), Harbin, China, was earned in 2008, and was promoted to Associate Prof. HIT, in 2012. This author became a Member (M) of The Chinese Society of Theoretical and Applied Mechanics (CSTAM) in 2010. Visiting researcher, Mechanics, KTH (2017-2018). The first author's major fields of study are focus on mechanics of flexible composite materials, membrane mechanics, and flexible structural mechniacs.

**Huifeng Tan**, Ph.D in Composite Materials, Harbin Institute of Technology (HIT), Harbin, China was earned in 1994, and was promoted to Associate Prof. HIT, in 2003.